

TIME DELAY BETWEEN IMAGES OF THE LENSED QUASAR UM673

E. Koptelova^{1,2,3}, W. P. Chen², T. Chiueh¹, B. P. Artamonov³, V. L. Oknyanskij³, S. N. Nuritdinov⁴,
O. Burkxonov⁴, T. Akhunov^{4,6}, V.V.Bruevich³, O.V. Ezhkova³, A.S.Gusev³, A.V.Sergeyev⁵,
Sh. A. Ehgamberdiev⁴, M. A. Ibragimov⁴

¹ Department of Physics, National Taiwan University, Taipei, Taiwan
[ekaterina;chiuehth]@phys.ntu.edu.tw

² Graduate Institute of Astronomy, National Central University, Jhongli City, Taiwan
wchen@astro.ncu.edu.tw

³ Sternberg Astronomical Institute (SAI), Moscow M.V. Lomonosov State University,
Moscow, Russia [artamon;oknyan]@sai.msu.ru

⁴ Ulugh Beg Astronomical Institute of the Uzbek Academy of Sciences, Tashkent,
Uzbekistan

ABSTRACT. We study brightness variations in the double lensed quasar UM673 (Q0142-100) with the aim of measuring the time delay between its two images. Methods.. We analyzed the *V*, *R* and *I*-band light curves of the A and B images of UM673, which cover ten observational seasons from August 2001 to November 2010. We also analyzed the time evolution of the difference in magnitudes (flux ratio) between images A and B of UM673 over more than ten years. We find that the quasar exhibits both short-term (with an amplitude of ~ 0.1 mag in the *R* band) and long-term (with an amplitude of ~ 0.3 mag) variability on timescales of about several months and several years, respectively. These brightness variations are used to constrain the time delay between the images of UM673. From a cross-correlation analysis of the A and B quasar light curves and an error analysis we measure a mean time delay of 89 days with an rms error of 11 days.

Multiple images of lensed quasars show changes in their brightness over time. There are two main reasons for these brightness variations. One is that the quasar itself, as a variable source, changes in brightness with time. Brightness variations of the quasar are observed in the light curves of all quasar images, but they are not synchronized. Changes in brightness in one image follow or lead the brightness changes in others with certain time lags (time delays). The time delay between these

brightness variations in any two images of the quasar is a combination of delays that arise from geometrical differences between the light paths (and thus light travel times) for each quasar image and the difference in the gravitational potential between quasar images. The geometrical term is related to the *Hubble* constant through the angular diameter distances (see Schneider et al. 1992). This relation gives us a method for estimating the *Hubble* constant independently of the distance ladder (Refsdal 1964). All references can see in Paper I and Paper II.

In this study we analyze brightness variations in images of the lensed system UM673 (Q0142-100) discovered by MacAlpine & Feldman (1982). The system consists of a distant quasar at redshift $z_q = 2.719$ (Surdej et al. 1987, 1988) gravitationally lensed by an elliptical galaxy at redshift $z_l = 0.49$ (Surdej et al. 1988; Smette et al. 1992; Eigenbrod et al. 2007) into A and B images with an image separation of $2''.2$. We used monitoring observations of UM673 obtained during different observational seasons at two sites. The majority of the observational data were collected during the quasar monitoring program carried out by the Maidanak GLQ collaboration (see Dudinov et al. 2000). The data were obtained with the 1.5-m AZT-22 telescope of the Maidanak Observatory (Central Asia, Uzbekistan) during the 1998–2010 observational seasons in the Bessel *V*, *R* and *I* bands. A considerable part of these observations, the 2003–2005 data, have been presented in Koptelova et al.

(2008) and Paper I. The V , R and I -band observations of the lensed system were also made between July 28, 2008 and January 18, 2010 using the 1.3-m SMARTS telescope at CTIO, Chile. These observations were part of the ToO observations carried out by National Central University, Taiwan. UM673 was usually observed from August until December, or sometimes January, when it was well visible at both sites. The resulting Maidanak and CTIO R -band light curves of the A and B quasar images are shown in Fig. 1. More details of photometric processing and results in V , I –band light can see in Koptelova et al. (2012), Paper II.

The time delay was measured with the modified cross-correlation function (MCCF) method (see Oknyanskij 1993). The method, its application and the test performance for the analysis of time series containing large annual gaps have been described in Paper I. Here, we briefly outline the approach. In the MCCF method, each data point from the B light curve, $B(t_i)$, forms a pair with an interpolated point from the A light curve, $A(t_i + \tau)$ at time $t_i + \tau$, where τ is the time lag. The pairs of data points for which $\tau - \Delta t \leq \Delta t_{ij} < \tau + \Delta t$ (where $\Delta t_{ij} = |t_j - t_i|$ is the time shift between the t_i point of the A light curve and the t_j point of the B light curve) are then used to calculate the cross-correlation function. The interpolation interval Δt is usually chosen as a compromise between the desire to decrease the interpolation errors and to find a sufficient number of data pairs to reliably calculate the correlation coefficient for a given time lag. For the analysis of the light curves presented in Paper I the value of Δt was adopted to be 90 days. This was the lowest value of Δt that one could choose because of the large annual gaps in the light curves of UM673. For this value of Δt the MCCF method is insensitive to brightness variations shorter than 90 days. Therefore the short-term variations of the quasar that are comparable to, or sometimes shorter than, the interpolation interval of 90 days, are ignored by the method. In addition, interpolation errors produced for high values of Δt can lead to an erroneous time delay estimate.

We used two interpolation intervals, Δt_{\max} and Δt_{\min} to account for the short-term variations in brightness and minimize the interpolation errors. The interpolation interval $\Delta t_{\max} = 90$ days is the same interval as was adopted for calculations of the CCF in Paper I. The interpolation interval Δt_{\min} was introduced to take into account the short-term brightness variations of UM673. It was used to calculate the cross-correlation function for those data pairs, for which both data points in the pair (the real point from the B light curve and the interpolated one from the A light curve) are within the same observational season. When the data points do not lie within the same season of observations, Δt_{\max} was used instead of Δt_{\min} . This approach was applied to calculate the cross-correlation function between the time-shifted interpolated A light curve and the discrete B light curve. The time lag ranges from -500 to 500 days with a step of 1 day. A value of 10 days chosen for Δt_{\min} is comparable to average sampling of the light curves within one observational season. The origin of the high-amplitude rapid brightness variation observed in image B in January 2010 is unclear. It can be either intrinsic to the quasar, with the

counterpart in image A that was missed, or unique for image B. To avoid the influence of the data points corresponding to this event on the correlation between the A and B light curves, these data were excluded from the time delay analysis. The resulting CCFs for the R , V and I -band data are shown in Figs. 4 and 5. (see Paper II). When observational data are regularly sampled and there is a good overlap between time-shifted light curves, interpolation can be avoided as in the method proposed by Pelt et al. (1994). In this method, the time delay is estimated by minimizing the dispersion spectrum of the combined A and time-delay-shifted B light curves. In the method, only pairs of data points within some interval, called the decorrelation length, contribute to the calculation of the dispersion spectrum. The dispersion spectra calculated for two values of the decorrelation length, 60 and 90 days, are shown in Fig. 6 by gray and black lines, respectively. We found only a tentative minimum in the global behavior of the dispersion spectra corresponding to a range of delays from 70 to 110 days. The shape of the minimum is not well constrained at longer delays, between 120 and 250 days. This region corresponds to the delays for which the A and B light curves do not overlap. Therefore, the method cannot be used to measure delays from this range. The minimum between 70 and 110 days consists of several secondary minima corresponding to different delays. We averaged the dispersion function in this range of time delays to estimate the location of its global minimum. The delay corresponding to the global minimum is 86 days in both cases, for values of the decorrelation timescale of 60 and 90 days. This estimate of the delay agrees with the time delay measured using the MCCF method. We found that in comparison with the dispersion function method, the MCCF method gives a more definite measurement of the delay. Uncertainties in time delay measurement due to photometric errors and systematic sampling effects were investigated with the Monte Carlo simulations. We performed simulations of 1000 artificial light curves using Timmer & Koenig's algorithm (1995) (these simulations are discussed in detail in Paper I). The distribution of the time delays recovered from cross-correlation analysis of the Monte Carlo simulated R -band light curves of images A and B, shifted by the input time delay of 88 days, is shown in Fig. 8 of Paper II. For this distribution we found a mean time delay of 89 (marked by a dotted line in Fig. 8) and an rms error of 11 days. On the other hand, the most probable value of the delay that can be measured from light curves with similar statistical properties and variability pattern as the observed R -band light is curves is 95 (+5/+14 and -16/-29) days (68% and 95% confidence intervals).

The measured time delay can be used to estimate the *Hubble* parameter and constrain the mass model of the lensing galaxy. There have been several lens models that predict different time delays between the UM673 images. The predicted time delay for the lens with elliptical symmetry and $H_0 = 75 \text{ km s}^{-1} \text{ Mpc}^{-1}$ is about 7 weeks (Surdej et al. 1988). Lehár et al. (2000) fitted a set of four standard lens models (SIE, constant M/L models, and those with external shear). The SIE and constant M/L models predict time delays of $h\Delta t = 80$ and $h\Delta t = 121$

days, respectively. The SIE and constant M/L models with external shear predict time delays of $h\Delta t = 84 \pm 87$ and $h\Delta t = 115$ days, respectively. Given that $\Delta t = 89$ days, the SIE and M/L models yield estimates of the *Hubble* constant H_{meas}^{-1} of 90 and 136 $\text{km s}^{-1} \text{Mpc}^{-1}$, respectively. The SIE and M/L models with shear yield values of H_{meas}^{-1} of 94 and 129 $\text{km s}^{-1} \text{Mpc}^{-1}$, respectively. These estimates of the *Hubble* constant are higher than the *Hubble* key project result of $72 \pm 8 \text{ km s}^{-1} \text{Mpc}^{-1}$ (Freedman et al. 2001) or improved result of $74.2 \pm 3.6 \text{ km s}^{-1} \text{Mpc}^{-1}$ (Riess et al. 2009). This might be due to an additional convergence to the lensing potential from nearby objects or objects on the line of sight to the quasar (see, e.g., Keeton et al. 2000). Leh'ar et al. (2000) estimated the total shear γT and convergence kT produced by nearby galaxies in the FOV of ten double lensed quasars observed with the *Hubble* Space Telescope (HST), including UM673. The total convergence from five galaxies within $20''$ of UM673 was estimated to be 0.138 (see Table 4 of Leh'ar et al. 2000). In the calculations Leh'ar et al. assumed that each galaxy has an SIS mass distribution, and their M/L ratios and redshifts are the same as for the lensing galaxy. Because of the assumptions made, the derived value of $k(T)$ can only be considered as approximate. For the SIS model, the *Hubble* parameter corrected for the field convergence of 0.138 as $H_0 = (1-k(T))^{-1}$, is $78 \pm 10 \text{ km s}^{-1} \text{Mpc}^{-1}$. This value roughly agrees within the errors with the *Hubble* key project value. The result can be improved even more when detail measurements of kT in the field of UM673 are available. An additional contribution to the total convergence produced by the objects on the line of sight to the quasar should also be investigated. Recently, Cooke et al. (2010) reported the discovery of a previously unrecognized DLA system at $z = 1.63$ in the spectrum of image A of UM673. They also found a weak Ly α

emission line in the spectrum of image B at the same redshift as the DLA that indicates a star formation rate of 0.2 solar mass per year. The discovery provides evidence for an additional mass, a galaxy that gives rise to the DLA system toward the UM673 quasar. The accuracy of the *Hubble* constant from the time delay in UM673 can be improved in the future by analyzing the external convergence produced by the objects in the FOV of UM673 and reducing the error in the time delay measurement. The latter requires coordinated observations of UM673 at different sites over the time interval that can provide better overlap between time-delay-corrected light curves of the quasar images than the Maidanak-CTIO data do. UM673 might exhibit rapid brightness variations of more than 0.1 mag on timescales from one to several months. Observations of these rapid brightness variations during coordinated monitoring of the system can help to reduce the uncertainty in the time delay down to several per cent.

References

- Dudinov V., Bliokh P., Paczynski B. et al.: 2000, *Kinematika i fizika nebesnyh tel*, **3**, 170.
 Koptelova, E., Shimanovskaya E., Artamonov B.: 2005, *MNRAS*, **356**, 323.
 Koptelova E. et al.: 2012, *A&A*, **544**, A51 (Paper II).
 Koptelova E.A., Oknyanskij V.L., Shimanovskaya E.V.: 2006, *A&A*, **452**, 37.
 Koptelova E.A., Artamonov B.P., Shimanovskaya E.V. et al.: 2007, *Astron. Rep.*, **51**, 797.
 Koptelova E., Artamonov B.P., Bruevich V.V., Burkhonov O.A., Sergeev A.V.: 2008, *Astron. Rep.*, **52**, 270.
 Koptelova E., Oknyanskij V.L., Artamonov B.P., Burkhonov O.: 2010, *MNRAS*, **401**, 2805 (Paper I).

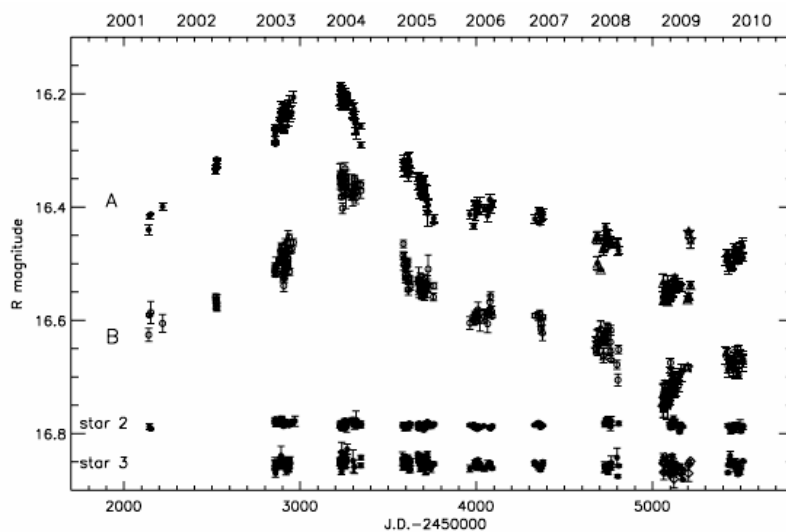


Figure 1: R-band light curves of the A and B images of UM673 from August 2001 to November 2010. For better representation, the light curve of image B is shifted by -1.87 mag. The light curves of reference stars 2 and 3 are shown at the bottom.